A Survivable and Flexible WDM Access Network by Alternate FSO- and Fiber-Paths for Fault Protection

Chien-Hung Yeh, *Member, IEEE*, Han-Shin Ko, Shien-Kuei Liaw, *Senior Member, IEEE*, Li-Hung Liu, Jing-Heng Chen, *Member, IEEE*, and Chi-Wai Chow, *Senior Member, IEEE*

***Abstract*—In the work, we study and express a new wavelength-division-multiplexing passive optical network (WDM-PON) architecture with fiber fault protection. The designed optical network unit (ONU) module and periodic spectrum of 2 × N array waveguide grating (AWG) are applied to produce the self-protected mechanism. Here, we employ the free space optical communication (FSO)- and fiber-based connection between two adjacent ONUs to achieve signal relink. Moreover, the corresponding signal performances of downstream and upstream are also analyzed and discussed.**

***Index Terms*—Free space optical communication (FSO), wavelength-division-multiplexing (WDM), fault protection, passive optical network (PON), on-off keying (OOK).**

I. Introduction

RECENTLY, due to the achievable demands of artificial intelligence (AI), cloud access, multi-service, big-data, 4K/8K video, and the online game, the reliable wavelength-division-multiplexing passive optical networks (WDM-PONs) should be an essential topic for higher capacity signal connection [1], [2]. Under such high-speed and broadband WDM access, the fiber breakpoint, which happens at the feeder and distribution fibers, would cause signal interruption [3]. The flexible and survivable fiber network architectures in such PON have been proposed and demonstrated [4]–[8].

Combining fiber access and free-space optical (FSO) communication has become a hot development issue [9], [10]. Due to some geographical or environmental constraints, the FSO connection can replace the fiber deployment in PON [9]. Furthermore, the FSO traffic in fiber networks could provide the benefits of reliable and flexible links, elastic bandwidth, innovative routing applications, various topology networks, and low cost [11], [12]. Sometimes due to special terrain restrictions or the cost fiber deployment, using wireless FSO connection in PON architecture will be an alternative. To achieve the survivable and flexible access operation, the several blended FSO and fiber link methods in PON architectures have been proposed recently [8], [13]–[15]. In 2020, Yeh *et al.* first demonstrated bidirectional 10 Gbit/s/λ on-off keying (OOK) ring-topology PON network by using time-division-multiplexing (TDM)-FSO access through 50 km fiber and 260 m FSO transmissions between two optical network units (ONUs) for fault protection [13], [14]. Then, Mirza *et al.* simulated a 5 Gbit/s/λ OOK self-protected polarization division multiplexing (PDM) WDM-PON with dual-path for fiber and FSO links between remote node (RN) and ONU for prevention [15]. This simulation results only displayed the ideal case for FSO and fiber transmission without the control mechanism of dual-polarization in real PON system. Moreover, the presented fiber-FSO based routing path maybe caused a fiber breakpoint. In 2021, Hayle *et al.* only exhibited the 10 Gbit/s/λ OOK FSO connection in WDM system through 25 km fiber link for PON protection [8]. However, they didn't demonstrate the FSO link length in presented network.

In the demonstration, we express and experimentally investigate a self-protected WDM-PON network against fiber breakpoint by using FSO- and fiber-based routing paths depending on the available deployment environments. To reduce the complexity of fault protection, we propose a simple ONU scheme and apply the optical periodicity of the array waveguide grating (AWG) to switch the routing path for signal reconnection. We utilize four downstream and four upstream wavelengths with 10 Gbit/s on-off keying (OOK) modulation in the self-protected fiber network for demonstration. After 50 km long-haul single-mode fiber (SMF) and 2 m FSO connections, all the optical signals can meet with the forward error correction (FEC) at the bit error rate (BER) of $\leq 3.8 \times 10^{-3}$. Besides, the available power budgets of 33.5 to 42.5 dB and 35.5 to 45 dB are also exhibited, when the fiber- and FSO-based protection of two adjacent ONUs are applied, respectively. Therefore, after 50 km SMF transmission, the free space link lengths of 220 to 880 m also can be reached based on the obtained redundant power.

II. Experiment and Discussions

Fig. 1(a) exhibits the presented tree-topology WDM-PON architecture with alternative FSO- and fiber-paths against fiber fault. In the optical line termination (OLT), we apply a 2 × N array waveguide grating (AWG) multiplexer (MUX) to connect

Manuscript received October 5, 2021; revised December 16, 2021; accepted December 29, 2021. Date of publication January 6, 2022; date of current version January 11, 2022. This work was supported by the Ministry of Science and Technology, Taiwan under Grants MOST-110-2221-E-035-058-MY2, MOST-110-2224-E-001-004, and MOST-109-2221-E-035-071. *(Corresponding author: Chien-Hung Yeh.)*

Chien-Hung Yeh, Han-Shin Ko, Li-Hung Liu, and Jing-Heng Chen are with the Department of Photonics, Feng Chia University, Taichung 40724, Taiwan (e-mail: yeh1974@gmail.com; xzbc699@gmail.com; jk1992581@gmail.com; jhchen@fcu.edu.tw).

Shien-Kuei Liaw is with the Department of Electronics and Computer Engineering, National Taiwan University of Science and Technology, Taipei 106335, Taiwan (e-mail: skliaw@mail.ntust.edu.tw).

Chi-Wai Chow is with the Department of Photonics, National Yang Ming Chiao Tung University, Hsinchu 30010, Taiwan (e-mail: cwchow@faculty.nctu.edu.tw).

Digital Object Identifier 10.1109/JPHOT.2021.3140095

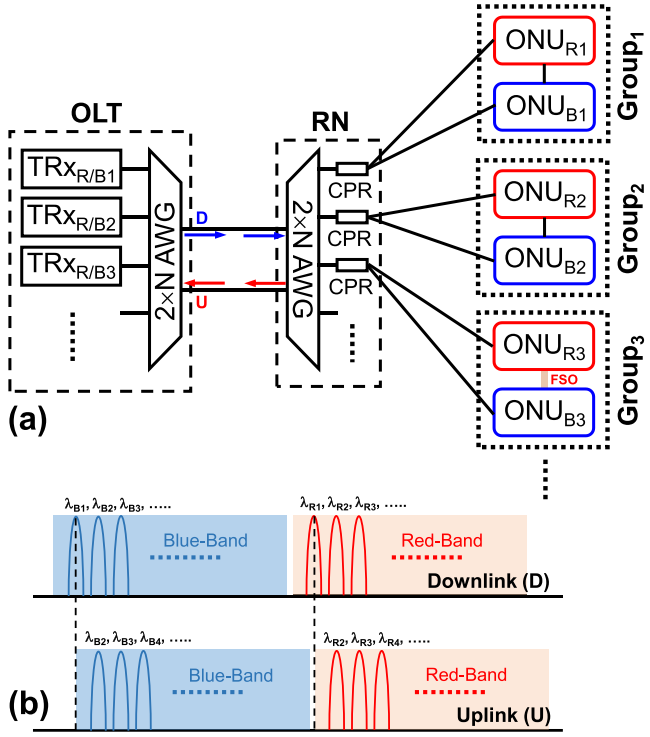

Fig. 1. (a) Presented self-protected WDM-PON architecture. (b) The periodic wavelength arrangement of 2 × N AWG.

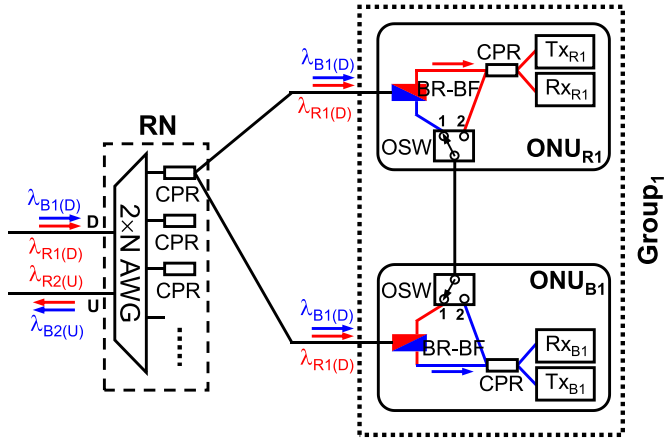

Fig. 2. Detailed schematic of the RN and ONU group1 under normal link status.

to each corresponding downstream wavelength. As seen in Fig. 1(b), the available bandwidth of downstream wavelengths can be divided into the red- and blue-bands, respectively. Thus, each connected port of 2 × N AWG can link two optical transceivers ($\mathrm{TRx_{R/B}}$) with two wavelengths of λ_{R1} and λ_{B1}, λ_{R2} and λ_{B2}, … and $\lambda_{\mathrm{R}N}$ and $\lambda_{\mathrm{B}N}$, respectively, based on the periodic spectrum of AWG. Then, the entire downstream wavelengths can be integrated into the "D" connected port for delivering. After a transmission length of single-mode fiber (SMF), all the downstream traffics are into the 2 × N AWG demultiplexer (DEMUX) for splitting to connect to each ONU at the remote node (RN). Next, a pair of downstream wavelengths of λ_{R1} and λ_{B1}, λ_{R2} and λ_{B2}, … and λ_{RN} and λ_{BN} will be arranged to the corresponding output port of AWG, respectively. Every pair of downstream signals can be split via a 1 × 2 optical coupler (CPR) and then into the $\mathrm{ONU_R}$ and $\mathrm{ONU_B}$ simultaneously, as illustrated in Fig. 1(a). This means that each output port of AWG at the RN can produce the N groups of ONUs. Although the $\lambda_{\mathrm{R(D)}}$ and $\lambda_{\mathrm{B(D)}}$ will enter the $\mathrm{ONU_R}$ and $\mathrm{ONU_B}$ at the same time, a blue-red bandpass filter (BR-BF) is applied in the $\mathrm{ONU_R}$ and $\mathrm{ONU_B}$ to permit the matching wavelength for passing and avoid the signal interference.

Furthermore, the "U" connected port of 2 × N AWG only permits the corresponding wavelengths of λ_{R2} and λ_{B2}, λ_{R3} and λ_{B3}, … and $\lambda_{\mathrm{R}(N+1)}$ and $\lambda_{\mathrm{B}(N+1)}$ for upstream traffic, respectively, as indicated in Figs. 1(a) and 1(b). Then, we can use these wavelengths in each ONU group serving as the upstream signals. Thus, the $\mathrm{ONU_{R1}}$ and $\mathrm{ONU_{B1}}$ will have the downstream and upstream channels of λ_{R1} and λ_{R2} and λ_{B1} and λ_{B2} to be regarded as the $\mathrm{Group_1}$, respectively. Identically, the N-th Group of $\mathrm{ONU_{R}}N$ and $\mathrm{ONU_{B}}N$ also have downstream and upstream signals of $\lambda_{\mathrm{R}N}$ and $\lambda_{\mathrm{R}(N+1)}$ and $\lambda_{\mathrm{B}N}$ and $\lambda_{\mathrm{B}(N+1)}$, respectively, as illustrated in Figs. 1(a) and 1(b). In the demonstration, due to two different downstream and upstream wavelengths in the WDM-PON system, the Rayleigh backscattering (RB) beat noise also can be avoided [10].

To achieve self-healing protection, each $\mathrm{ONU_R}$ and $\mathrm{ONU_B}$ can be connected by the SMF- or FSO-based link to prevent the fiber breakpoint occurring between RN and ONU, as viewed in Fig. 1(a). Thus, the detailed protection schematic of the ONU group is schemed in Fig. 2. Here, we assume that the adjacent $\mathrm{ONU_{R1}}$ and $\mathrm{ONU_{B1}}$ are the $\mathrm{Group_1}$. A 1 × 2 optical switch (OSW), a BR-BF, a CPR, and the corresponding optical transmitter (Tx) and receiver (Rx) are exploited in the $\mathrm{ONU_{R1}}$ and $\mathrm{ONU_{B1}}$, respectively. Here, a length of SMF is employed to connect the $\mathrm{ONU_{R1}}$ and $\mathrm{ONU_{B1}}$, as seen in Fig. 2. In a typical operation, the downstream λ_{R1} and λ_{B1} from the "D" point of AWG can enter corresponding ONU for decoding downstream signal via the BR-BF, when the OSWs are both switched to the "1" point. Furthermore, the upstream λ_{R2} and λ_{B2} from $\mathrm{ONU_{R1}}$ and $\mathrm{ONU_{B1}}$ can transmit through the same path and output from the "U" point of AWG, as exhibited in Fig. 2.

In the normal state of signal access, all the OSW is connected to the "1" point. Besides, the downstream traffic is continuously transmitted to ONU. If a fiber fault appears at the point of Fig. 3 suddenly, the data connection between RN and $\mathrm{ONU_{R1}}$ will be interrupted. At this moment, the $\mathrm{Rx_1}$ of $\mathrm{ONU_{R1}}$ cannot detect the corresponding downstream signal. Then, the media access control (MAC) layer can switch the OSW to "2" point for signal reconnection by the fiber protection path through the $\mathrm{ONU_{B1}}$, as exhibited in Fig. 3. When the fiber breakpoint is repaired, the OSW can be switched back to position "1". This means that the OSW switching is based on whether the $\mathrm{Rx_1}$ has received downstream channel. Hence, we don't need to add the extra monitoring devices for switching in the presented PON. Similarly, if a fault occurs between RN and $\mathrm{ONU_{B1}}$, the transmission signal would also relink through the $\mathrm{ONU_{R1}}$, as shown in Fig. 3.

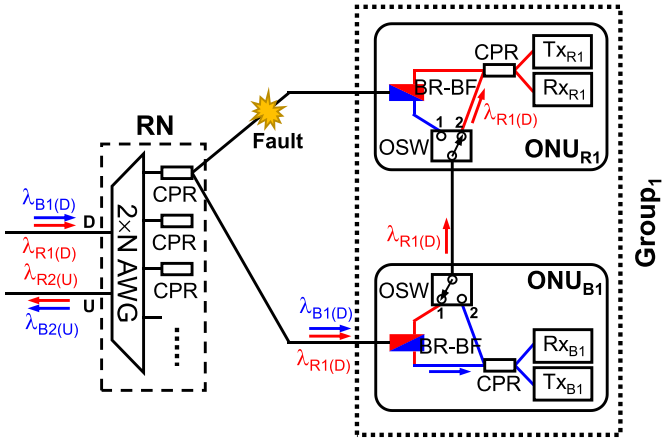

Fig. 3. The bidirectional signal transmission by the routing fiber path, when a fault is occurring between the RN and ONU$_{R1}$.

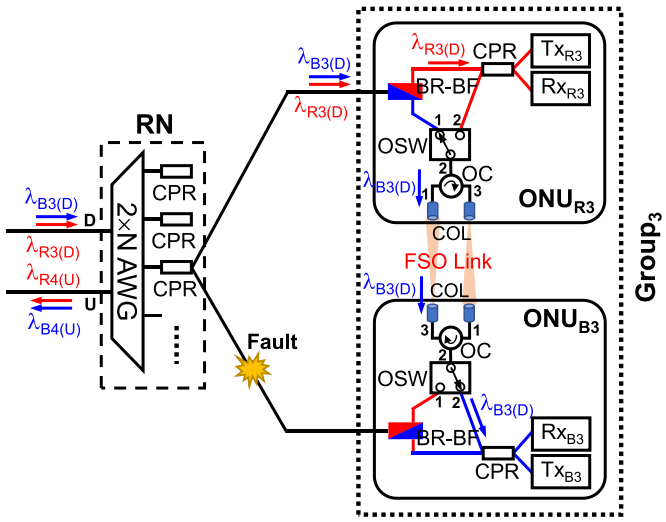

Fig. 4. The bidirectional signal transmission by the routing FSO path occurs when a fault between the RN and ONU$_{B3}$.

Furthermore, it is challenging to deploy optical fiber for data connection owing to the environment or special restrictions [7], [9]. Using the FSO connections will be another option. Thus, we also can utilize the FSO technique in the proposed self-protected ONU modules, as illustrated in Fig. 4. Here, we suppose the FSO connection is built between the ONU$_{R3}$ and ONU$_{B3}$. In order to generate the FSO transmission, the extra optical devices of two fiber-type collimators (COLs) and an optical circulator (OC) are added to distinguish and deliver the downstream and upstream signals, respectively, as shown in Fig. 4. As mentioned above, the OSW of each ONU is initially linked to a "1" point, when there is no fiber breakpoint between RN and ONU. Correspondingly, if a breakpoint occurs between the RN and ONU$_{B3}$, the Rx$_{B3}$ of ONU$_{B3}$ cannot receive any signal at once. The OSW will switch to the "2" point for reconnection at once by the FSO method to reconnect the signal traffic, as plotted in Fig. 4. Hence, the downstream λ_{B3} and upstream λ_{B4} can be relinked via the alternative FSO path.

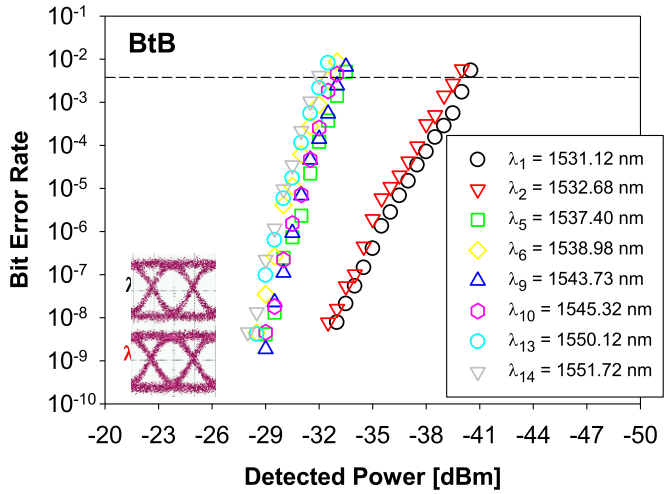

Fig. 5. Measured 10 Gbit/s OOK BER performances of eight selected wavelengths from λ_1 to λ_{14} at the BtB status.

Then, to understand the bidirectional signal performances in the self-protected PON system, we can apply 2×4 AWG in the experiment first. To generate two ONU Groups in the measurement, we utilize the wavelengths of 1531.12 ($\lambda_{1(D)}$), 1537.40 ($\lambda_{5(D)}$), 1543.73 ($\lambda_{9(D)}$) and 1550.12 nm ($\lambda_{13(D)}$), and 1532.68 ($\lambda_{2(U)}$), 1538.98 ($\lambda_{6(U)}$), 1545.32 ($\lambda_{10(U)}$) and 1551.72 ($\lambda_{14(U)}$) to regard as the downstream and upstream signals, respectively. Thus, the $\lambda_{1(D)}$ and $\lambda_{2(U)}$ and $\lambda_{5(D)}$ and $\lambda_{6(U)}$ are applied in the ONU$_{B1}$ and ONU$_{R1}$ to produce the Group$_1$, respectively. Besides, we also use the $\lambda_{9(D)}$ and $\lambda_{10(U)}$ and $\lambda_{13(D)}$ and $\lambda_{14(U)}$ to represent another Group here.

The experimental setup is according to the proposed WDM-PON network, as seen in Fig. 1(a) and Fig. 3. In the OLT, the various wavelengths are used to connect to the 10 GHz Mach-Zehnder modulator (MZM) for generating a 10 Gbit/s on-off keying (OOK) modulation signal with a pattern length of 2^{15}–1. The output power of each downstream wavelength is nearly 7.5 dBm after outputting the OLT. The downstream wavelength would pass through the RN and launch into the corresponding ONU after a transmission length of 50 km single-mode fiber (SMF). We also use the 10 Gbit/s OOK modulation in each ONU for upstream transmission and transmit through the same path for the data link. First, we execute the bit error rate (BER) performances of eight selected wavelengths at the back-to-back (B2B) state as above. As exhibited in Fig. 5, the measured eight power sensitivities of λ_1 to λ_{14} are –40, –39.5, –33, –32.5, –33, –32.5, –32, and –31.5 dBm under the forward error correction (FEC) level at the BER $\leq 3.8 \times 10^{-3}$, respectively. Besides, the insets are the eye diagrams of λ_1 and λ_2 at the minimum detected sensitivities of –33.5 and –33 dBm.

Next, we verify the 10 Gbit/s OOK BER measurements of the four downstream and four upstream traffics after passing through 50 km SMF transmission, respectively. Each upstream power of ONU is also set at 7.5 dBm. Fig. 6 presents the measured BER signals of $\lambda_{1(D)}, \lambda_{2(U)}, \lambda_{5(D)}, \lambda_{6(U)}, \lambda_{9(D)}, \lambda_{10(U)}, \lambda_{13(D)}$, and $\lambda_{14(U)}$ through 50 km SMF connection, respectively. To be below the FEC threshold, the reached power sensitivities are –35,

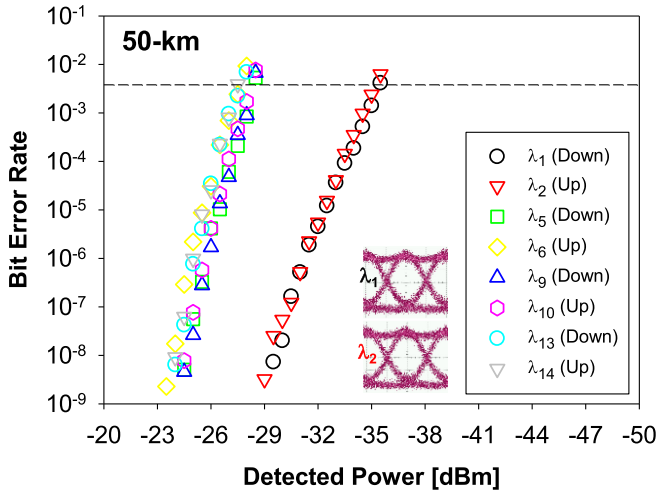

Fig. 6. Observed 10 Gbit/s OOK BER measurements of eight selected wavelengths from λ_1 to λ_{14} after 50 km SMF transmission. Insets are the observed eye diagrams of λ_1 and λ_2, respectively, at the most significant detected power.

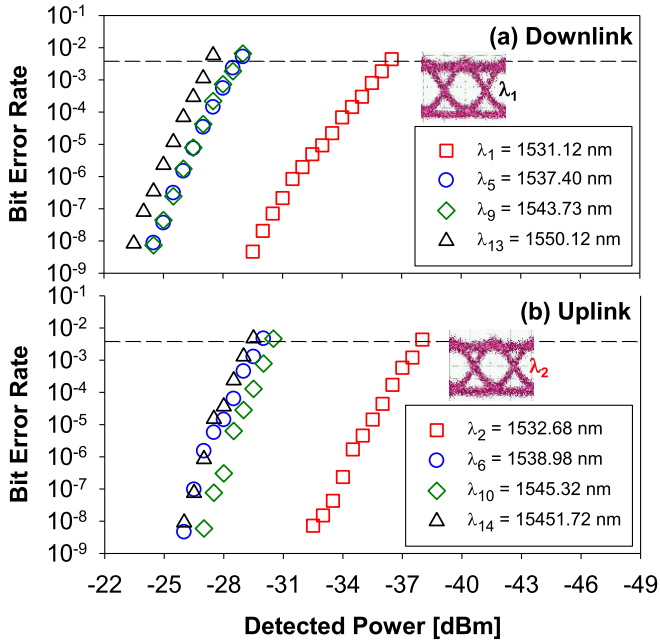

Fig. 7. Observed 10 Gbit/s OOK BER measurements of eight selected wavelengths from λ_1 to λ_{14} after 50 km SMF transmission. Insets are the observed eye diagrams of λ_1 and λ_2, respectively, at the most significant detected power.

–35, –28, –27.5, –28, –28, –27.5, and –27 dBm, respectively, as seen in Fig. 6. The insets are the observed eye diagrams of $\lambda_{1(D),}$ and $\lambda_{2(U)}$ at the minimum detected powers of –30 and –29.5 dBm (BER = 10^{-8}), respectively. Therefore, the power budgets of 42.5, 42.5, 35.5, 35, 35.5, 35.5, 35, and 33.5 dB are obtained at the eight selected wavelengths under the FEC target, respectively. Besides, the total insertion loss of 27 dB is caused by a 50 km SMF (0.2×50 = 10 dB), and AWG (6 dB), a 1×2 CPR (3 dB), a BR-BF (3 dB), a 2×2 CPR (3 dB), two OSWs (1+1 dB), when fiber-based protection is activated as seen in Fig. 3. As a result, all the achieved power budgets of downstream and upstream signals would be larger than that of insertion loss of 27 dB in the presented self-protected network after a 50 km SMF connection.

Finally, we use the FSO connection between ONU_R and ONU_B to confirm the performance of fault protection according to the setup of Fig. 4. Here, a 2 m free-space transmission length is set to simplify the FSO setup for optical wireless signal connection. Here, the diameter, focal length, and divergence angle of COL are 2 cm, 3.713 cm, and 0.016°, respectively. We also utilize the same eight selected wavelengths for bidirectional FSO demonstration. Besides, the detected FSO power loss among two COLs is close to 2.8 dB when an optimal alignment is achieved. So, the total insertion loss of 30.8 dB is caused by a 50 km SMF (0.2×50 = 10 dB), and AWG (6 dB), a 1×2 CPR (3 dB), a BR-BF (3 dB), a 2×2 CPR (3 dB), two OSWs (1+1 dB), two OCs (0.5+0.5 dB), and between two COLs (2.8 dB), respectively, while the FSO-based protection is operated in the pure atmosphere. The measured 10 Gbit/s OOK BER performances of four FSO downstream ($\lambda_{1(D)}$, $\lambda_{5(D)}$, $\lambda_{9(D)}$ and $\lambda_{13(D)}$) and upstream signals ($\lambda_{2(U)}$, $\lambda_{6(U)}$, $\lambda_{10(U)}$ and $\lambda_{14(U)}$) through 50 km SMF transmission and 2 m FSO connection, respectively, as exhibited in Figs. 7(a) and 7(b). The attained sensitivities of the downstream and upstream channels are –36, –28.5, –28.5, and –27 dBm and –37.5, –29.5, –30, and –29 dBm without dispersion compensation and optical amplification under the FEC level, respectively. The corresponding power budgets of 43.5, 36, 36, 34.5 dB and 45, 37, 37.5, and 36.5 dB are obtained, respectively. The insets are the observed eye diagrams of $\lambda_{1(D)}$ and $\lambda_{2(U)}$ at the detected powers of –29.5 and –32.5 dBm. In addition, we can estimate the achievable FSO transmission length based on the optical system design in the previous work [9]. The obtained redundant powers are between 3.7 to 14.2 dB in the BER measurement. Therefore, the FSO link lengths of 220 to 880 m will be reached based on the redundant power in the designed PON architecture when the atmosphere is assumed at a pure state. Here, to achieve FSO link, the optical components of two COLs and OC only are added in each ONU. So, the FSO technique can be used to replace special environments where fiber networks cannot be deployed. Essentially, the cost of fiber deployment is expensive than that of FSO link. As a result, we can perform fiber- or FSO-based fault protection operations based on actual needs.

In the previous studies [8], [15], [17], they needed to apply dual fiber paths to connect to two adjacent ONUs for avoid the fault of distribution fiber. And there was no clear design and description in Refs. [8] and [15] via FSO connection between two ONUs. Moreover, their designed ONU also required to add more device to achieve self-protected action. The presented WDM access network not only achieves the fiber breakpoint protection by using fiber path and FSO link simultaneously, but also uses fewer optical components in each ONU for simplifying network and providing cost-effectiveness.

Since both the downlink and uplink signals are at different wavelengths at the SMF, the RB from the downlink signal will not affect the uplink signal; hence Rayleigh beat noise can be avoided. On the other hand, since RB of light is due to the

randomly-distributed variations in the refractive index caused by inhomogeneities of the optical fiber, there will be no RB in the FSO since the transmission medium is air. Hence, the detected eye diagrams of two protection types are similar as shown in Figs. 6 and 7.

Unlike fiber loss, the RB will only produce backward optical noise. Based on the study in Ref. [18], the RB optical noise will be about –20 dB of the input signal produced by a 20 km standard SMF. The RB noise will have the same wavelength as the input signal. The signal degradation depends on the optical-signal-to-Rayleigh-noise-ratio (OSRNR) as discussed in Ref. [18]. When the OSRNR is < 25 dB, this means the optical signal is 25 dB less than the RB noise, 1 dB power penalty will be observed. In the experiment shown in Fig. 1(a), since both the downlink and uplink signals are at different wavelengths, the RB from the downlink signal will not affect the uplink signal; hence Rayleigh beat noise can be avoided.

III. Conclusion

We expressed and demonstrated a self-protected WDM-PON architecture with fault protection. The designed ONU module and the wavelength periodicity of 2×N AWG at the RN were applied in the presented WDM network to prevent the fiber breakpoint. In the experiment, eight WDM wavelengths were applied to produce two pairs of ONU Groups for self-protected operation. The fiber- and FSO-based connections between two adjacent ONUs were demonstrated against fiber fault. Here, 10 Gbit/s OOK modulation were applied on both downstream and upstream signals for BER observations. All the 10 Gbit/s data rates could meet with the FEC target (BER $\leq 3.8\times10^{-3}$) after 50 km long-haul SMF transmission and 2 m FSO wireless link. In addition, according to the redundant power of WDM signal, the free space link lengths of 220 to 880 m could be reached based on the previous optical design without optical amplification when the atmosphere was set at pure status. As a result, the proposed WDM-PON system with fault protection was not only simple, but also provided alternative signal links by the fiber- and FSO-based ways between two ONUs.

References

[1] L. Zhou, H. He, Y. Zhang, Y. Chen, Q. Xiao, and Z. Dong, "Enhancement of spectral efficiency and power budget in WDN-PON employing LDPC-coded probabilistic shaping PAM8," *IEEE Access*, vol. 8, pp. 45766–45773, 2020.

[2] J. Zhou *et al.*, "8 × 10 Gb/s downstream PAM-4 transmission for cost-effective coherent WDM-PON application," *J. Lightw. Technol.*, vol. 39, no. 9, pp. 2837–2846, May 2021.

[3] X. Sun, C.-K. Chan, and L.-K. Chen, "A survivable WDM PON with alternate-path switching," in *Proc. Opt. Fiber Conf.*, 2006, Paper JThB71.

[4] H. Erkan, G. Ellinas, A. Hadjiantonis, R. Dorsinville, and M. Ali, "Native Ethernet-based self-healing WDM-PON local access ring architecture: A new direction for supporting simple and efficient resilience capabilities," in *Proc. IEEE Int. Conf. Commun.*, 2010, pp. 1–6.

[5] J.-Y. Kim, S.-G. Mun, H.-K. Lee, and C.-H. Lee, "Self-restorable WDM-PON with a color-free optical source," *J. Opt. Commun. Netw.*, vol. 1, no. 6, pp. 565–570, Nov. 2009.

[6] Y. Qiu, Z. Liu, and C.-K. Chan, "A centrally controlled survivable WDM-PON based on optical carrier suppression technique," *IEEE Photon. Technol. Lett.*, vol. 23, no. 6, pp. 386–388, Mar. 2011.

[7] C.-H. Yeh, C.-M. Luo, Y.-R. Xie, C.-W. Chow, Y.-W. Chen, and T.-A. Hsu, "Survivable and reliable WDM-PON system with self-protected mechanism against fiber fault," *IEEE Access*, vol. 7, pp. 165088–165092, 2019.

[8] S. T. Hayle *et al.*, "Integration of fiber and FSO network with fault-protection for optical access network," *Opt. Commun.*, vol. 484, 2021, Art. no. 126676.

[9] C.-H. Yeh, B.-S. Guo, C.-S. Gu, C.-W. Chow, and W.-P. Lin, "Use of same WDM channels in fiber network for bidirectional free space optical communication with Rayleigh backscattering interference alleviation," *IEEE Access*, vol. 7, pp. 169571–169576, 2019.

[10] C.-H. Yeh, J.-R. Chen, W.-Y. You, and C.-W. Chow, "Hybrid WDM FSO fiber access network with Rayleigh backscattering noise mitigation," *IEEE Access*, vol. 8, pp. 96449–96454, 2020.

[11] C.-L. Ying, H.-H. Lu, C.-Y. Li, C.-A. Chu, T.-C. Lu, and P.-C. Peng, "A bidirectional hybrid lightwave transport system based on fiber-IVLLC and fiber-VLLC convergences," *IEEE Photon. J.*, vol. 7, no. 4, Aug. 2015, Art. no. 7201611.

[12] H.-W. Wu, C.-Y. Li, H.-H. Lu, Q.-P. Huang, S.-C. Tu, and Y.-C. Huang, "A PDM-based 128-Gb/s PAM4 fibre-FSO convergent system with OBPFs for polarisation de-multiplexing," *Sci. Rep.*, vol. 10, no. 1, pp. 1–9, 2020.

[13] C.-H. Yeh, Y.-R. Xie, C.-M. Luo, and C.-W. Chow, "Integration of FSO traffic in ring-topology bidirectional fiber access network with fault protection," *IEEE Commun. Lett.*, vol. 24, no. 3, pp. 589–592, Mar. 2020.

[14] C.-H. Yeh *et al.*, "Fiber- and FSO-protected connections for long-reach TWDM access architecture with fault protection," *IEEE Access*, vol. 8, pp. 189982–189988, 2020.

[15] J. Mirza, W. A. Imtiaz, A. J. Aljohani, A. Atieh, and S. Ghafoor, "Design and analysis of a 32× 5 Gbps passive optical network employing FSO based protection at the distribution level," *Alex. Eng. J.*, vol. 59, no. 6, pp. 4621–4631, 2020.

[16] J. W. Simatupang and S.-L. Lee, "Transfer matrix analysis of backscattering and reflection effects on WDM-PON systems," *Opt. Exp.*, vol. 21, no. 23, pp. 27565–27577, 2013.

[17] Z. Wang, X. Sun, C. Lin, C.-K. Chan, and L.-K. Chen, "A novel centrally controlled protection scheme for traffic restoration in WDM passive optical networks," *IEEE Photon. Technol. Lett.*, vol. 17, no. 3, pp. 717–719, Mar. 2005.

[18] C. W. Chow, G. Talli, and P. D. Townsend, "Rayleigh noise reduction in 10-Gb/s DWDM-PONs by wavelength detuning and phase-modulation-induced spectral broadening," *IEEE Photon. Technol. Lett.*, vol. 19, no. 6, pp. 423–425, Mar. 2007.